

# RSC Advances



This is an *Accepted Manuscript*, which has been through the Royal Society of Chemistry peer review process and has been accepted for publication.

*Accepted Manuscripts* are published online shortly after acceptance, before technical editing, formatting and proof reading. Using this free service, authors can make their results available to the community, in citable form, before we publish the edited article. This *Accepted Manuscript* will be replaced by the edited, formatted and paginated article as soon as this is available.

You can find more information about *Accepted Manuscripts* in the [Information for Authors](#).

Please note that technical editing may introduce minor changes to the text and/or graphics, which may alter content. The journal's standard [Terms & Conditions](#) and the [Ethical guidelines](#) still apply. In no event shall the Royal Society of Chemistry be held responsible for any errors or omissions in this *Accepted Manuscript* or any consequences arising from the use of any information it contains.



## Characteristics of phospholipid DOPC/cholesterol bilayer in aspect of surface free energy and its components

M. Jurak<sup>a</sup> and E. Chibowski

Received 00th January 20xx,  
Accepted 00th January 20xx

DOI: 10.1039/x0xx00000x

www.rsc.org/

The effect of cholesterol (Chol) content ( $x_{\text{Chol}} = 0.25; 0.5; 0.75$ ) on wettability changes of solid supported bilayers of unsaturated 1,2-dioleoyl-*sn*-glycero-3-phosphatidylcholine (DOPC) was investigated at 20°C and 37°C. The effect was determined via changes of the film's apparent surface free energy and its components. The energy changes were calculated from the measured apparent advancing contact angles. The obtained results demonstrate that the amount of cholesterol in DOPC bilayers influence the film surface free energy and especially the electron-donor component. The changes depend on the system temperature but are not linear relative to cholesterol content. Also the surface roughness of the DOPC/Chol surface was determined by atomic force microscopy (AFM). The average roughness, root-mean-square roughness and average height parameters showed that up to  $x_{\text{Chol}} = 0.5$  the surfaces were very smooth (subnanometer roughness). At  $x_{\text{Chol}} = 0.75$  the phase separation occurred with visible cholesterol islands (domains) and the roughness parameters have increased to 3–4.8 nm. This allows preparation of the film surfaces of targeted properties which would have potentially practical applications.

### Introduction

The principal role of cholesterol in biological membrane relays on its stiffening and ordering, thus causing strengthening the interactions between individual components. This makes the membrane more stable and lowers its permeability to water and other molecules.<sup>1,2</sup> However, cholesterol exhibits solubility limit in DOPC bilayer and if its amount exceeds the limit the excess of it precipitates as monohydrate crystals,<sup>3</sup> or within the membrane immiscible cholesterol bilayer domains are formed.<sup>4</sup> The domains may play positive physiological role, for example maintaining eye lens transparency thus protecting against cataract.<sup>5,6</sup> Moreover, an increase of the total cholesterol/phospholipid molar ratio occurs with ageing.<sup>7</sup> Since cholesterol is present in large amount in animal plasma membranes, it is significant to learn about its effects on the structure (molecular organization), fluidity and permeability of bilayers composed of phospholipids, as well as to understand the formation of cholesterol-rich domains in biomembranes. On the other hand, for membranes temperature is thermodynamic parameter that determines critical thermal fluctuations,<sup>8</sup> phase transitions,<sup>9</sup> and domain formation.<sup>10</sup> The temperature effect is revealed to a great extent through the disordering of hydrocarbon chains. The presence of cholesterol in DOPC bilayer strongly influences the nature of the lamellar phase by changing ordering of DOPC molecules from

disordered to ordered liquid-crystalline phase.<sup>11</sup> This phase is similar to the gel phase with less lateral packing order and simultaneously to the fluid phase with more packing order. Plesnar et al. using an atomistic MD simulation method pointed out that saturation of DOPC bilayer with Chol significantly narrows the distribution of vertical positions of each lipid atom at all the bilayer depths which becomes smoother.<sup>12</sup>

The planar bilayer structure is in mutual balance between lateral attractive and repulsive forces, including hydrophobic, van der Waals, steric, dipole–dipole and electrostatic interactions if present. The surface properties and especially the surface free energy and its components of model biological membranes can be helpful in understanding of the interactions mechanism responsible for the stability of molecular films, molecular reorganization, wetting, spreading, and permeability in the biomedical applications. Therefore understanding of these interfacial phenomena requires knowledge about not only the total surface free energy but also its components resulting from different kind and strength of the forces acting across the interface.

The wetting properties of a solid surface are often determined via measurement of contact angle  $\theta$  of a water droplet settled on the surface. The contact angle is a directly measured quantity which reflects the competition between the energy of cohesion of liquid molecules and the energy of adhesion between the liquid and solid, that is the interactions (forces) acting along the three phase (solid/liquid/gas) contact line. In fact, the water contact angle is a parameter to measure solid surface hydrophobicity. Water being a highly polar liquid, aside from ever-present London dispersive forces (21.8 mN/m), interacts by strong polar Lewis acid-base forces (51.0 mN/m) (Table 1). The latter ones are the electron-donor and electron-acceptor interactions, here originating from water ability to hydrogen bonding formation, both as the donor and acceptor of

<sup>a</sup> Department of Physical Chemistry, Faculty of Chemistry, Maria Curie-Skłodowska University, 20-031 Lublin, Poland, Phone: +48 – 81 5375547, Fax: +48 – 81 5333348, E-mail address: [malgorzata.jurak@poczta.umcs.lublin.pl](mailto:malgorzata.jurak@poczta.umcs.lublin.pl)

† Footnotes relating to the title and/or authors should appear here. Electronic Supplementary Information (ESI) available: [details of any supplementary information available should be included here]. See DOI: 10.1039/x0xx00000x

electrons. Hence, the higher the contact angle is, the more hydrophobic the solid surface is. However, to evaluate the apolar and polar acid-base interactions for given solid surface, it is necessary to measure contact angles with three different liquids of which at least two must be polar (e.g. water and formamide) and the third apolar (e.g. diiodomethane). Then applying theoretical approach proposed by van Oss, Good and Chaudhury,<sup>13-16</sup> called Lifshitz-van der Waals/Acid-Base (LWAB) model one can calculate the components of surface free energy. In this approach it is assumed<sup>13-16</sup> that the surface free energy is the sum of the apolar Lifshitz-van der Waals component  $\gamma_S^{LW}$  and the polar Lewis acid-base  $\gamma_S^{AB}$  component (the electron-donor  $\gamma_S^-$  and electron-acceptor  $\gamma_S^+$  parameters):

$$\gamma_S^{tot} = \gamma_S^{LW} + \gamma_S^{AB} = \gamma_S^{LW} + 2\sqrt{\gamma_S^- \gamma_S^+} \quad (1)$$

Then the work of adhesion  $W_A$  of a liquid to the solid surface can be expressed as follows:

$$W_A = \gamma_L(1 + \cos\theta_a) = 2\sqrt{\gamma_S^{LW} \gamma_L^{LW}} + 2\sqrt{\gamma_S^+ \gamma_L^-} + 2\sqrt{\gamma_S^- \gamma_L^+} \quad (2)$$

where the subscripts 'S' and 'L' mean solid and liquid, respectively, and  $\theta_a$  is the advancing contact angle of the probe liquid.

It should be emphasized that Eq. 2 contains three unknowns,  $\gamma_S^{LW}$ ,  $\gamma_S^+$ , and  $\gamma_S^-$ , and the values of surface free energy components of liquids,  $\gamma_L^{LW}$ ,  $\gamma_L^+$ , and  $\gamma_L^-$ , have to be known (Table 1).<sup>15,17,18</sup> To determine the components of surface free energy and then its total value, the three equations of Eq. 2 type should be solved simultaneously.

**Table 1.** Surface tension and its components (in  $\text{mJ/m}^2$ ) of the probe liquids in  $\text{mJ/m}^2$ .<sup>15,17,18</sup>

Probe liquid	Temp. °C	$\gamma_L$	$\gamma_L^{LW}$	$\gamma_L^{AB}$	$\gamma_L^+$	$\gamma_L^-$
Water, H <sub>2</sub> O	20	72.8	21.8	51.0	25.5	25.5
	37	70.3	20.3	50.0	25.0	25.0
Formamide, HCONH <sub>2</sub>	20	58.0	39.0	19.0	2.28	39.6
	37	55.1	36.7	18.4	2.2	38.3
Diiodomethane, CH <sub>2</sub> I <sub>2</sub>	20	50.8	50.8	0.0	0.0	0.0
	37	48.1	48.1	0.0	0.0	0.0

Moreover, it should be stressed that the LWAB theory does not include the contribution of electrostatic interactions in surface free energy of liquids and solids, and there is no other theory and experimental procedure, with a help of which one would determine the electrostatic interactions via contact angle measurements. This can be done using DLVO (Derjaguin, Landau, Verwey and Overbeek) theory of colloidal particles stability, but it is not appropriate in the case of liquid drop/solid interface.

In terms of Lewis approach, the acid-base ( $\gamma^{AB}$ ) component, in principle, is dealing with hydrogen bonding and  $\pi$  electron pairs (Fig. 1). The polar interactions  $\gamma^{AB}$  in most cases are due to the formation of hydrogen bonds between the hydrogen and oxygen, as well as the other electron-donor atoms. The hydrogen bond may be considered as the Lewis acid-base interaction between the electron-acceptor (acid) and the electron-donor (base). Accordingly, the

$\gamma^{AB}$  component is the geometric mean of the electron-donor ( $\gamma^-$ ) and the electron-acceptor ( $\gamma^+$ ) parameter (Eq. 1).

On the other hand, according to the authors of this approach<sup>13-16</sup> the apolar component  $\gamma^{LW}$ , beyond principal London dispersion interactions, includes minor dipole-dipole interactions (Keesom forces) and dipole-induced dipole interactions (Debye forces) but their contribution does not exceed 3% of the apolar component.

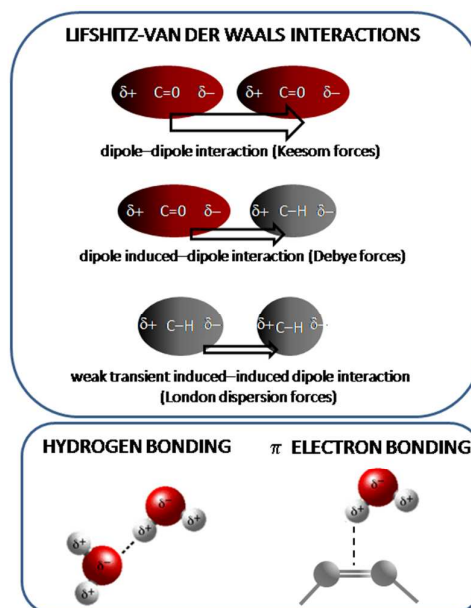


**Fig. 1** Types of interactions involved in the LWAB theory.

Although this is the most often used approach for solid surface free energy, it has also some shortages. This will be discussed later. Unfortunately, problem of solid surface free energy determination is not yet solved completely. Nevertheless, even the apparent values calculated from the LWAB approach deliver interesting information on changes in the investigated surface interactions.

The purpose of this paper was investigation how the wettability (hydrophobic/hydrophilic properties) of model DOPC/Chol lipid bilayers, supported on mica, is influenced by temperature and the layers composition, i.e. the ratio of these two lipid components. The molar fraction of cholesterol in DOPC bilayer was  $x_{\text{Chol}} = 0.25, 0.5$  or  $0.75$ . The experiments were conducted at room ( $20^\circ\text{C}$ ) and physiological ( $37^\circ\text{C}$ ) temperatures. Moreover, structure of the studied bilayers was confirmed by atomic force microscopy (AFM) technique. We hope that the results may be helpful for better understanding of wetting processes taking place in native biological membranes, possibly better understanding how the cells adjustment to their external environment can be achieved. Some practical meaning of the results for preparation of surfaces of demanded hydrophilicity can be thought.

## Experimental

### Materials

1,2-Dioleoyl-*sn*-glycero-3-phosphatidylcholine (DOPC, synthetic, 99%) and cholesterol (Chol, 99%) were purchased from Sigma and used without any further purification. Chloroform  $\text{CHCl}_3$  (p.a.) used

as the solvent for lipids was supplied by POCH S.A., Poland. The water used in this study was purified by a Milli-Q Plus system (Millipore, USA) with resistivity 18.2 M $\Omega$ cm. The probe liquids used for contact angle measurements were: pure water, formamide (98 %, Aldrich) and diiodomethane (99 %, Aldrich). The support for the bilayer deposition was freshly cleaved muscovite (Continental Trade, Poland) cut as plates of 38 mm  $\times$  26 mm  $\times$  0.5 mm size.

#### Preparation of Supported Lipid Bilayers

The Langmuir-Blodgett/Langmuir-Schaefer (LB/LS) technique was applied to prepare the solid supported lipid bilayers. A 1 mg/mL solution of lipid or binary mixture (DOPC/Chol) in CHCl<sub>3</sub> was spread at the air/water interface of a Langmuir-Blodgett trough (KSV 2000, Finland) equipped with two symmetrical barriers and Wilhelmy plate for the surface pressure measurements. The mixed (DOPC/Chol) solutions of defined composition ( $x_{\text{Chol}} = 0.25; 0.5; 0.75$ ) were prepared from the respective stock solutions. The subphase temperature (20°C or 37°C) was controlled thermostatically by a circulating water system. After spreading the monolayers were left to equilibrate for 10 min before the compression was initiated with the barrier speed of 10 mm/min. The first layer was deposited on the mica plate via a vertical pull out from the aqueous subphase into air. After 15 min the second layer was deposited using the LS method by horizontal touching the mica with already deposited monolayer to the subphase. The transfer of all LB and LS films was carried out at the surface pressure of 35 mN/m at 20°C or 37°C. After deposition the lipid bilayers were placed in a vacuum desiccator (Binder) and dried under the pressure of 117 mbar for about 18–20 h.

#### Contact angle measurements

Measurements of advancing contact angles of the probe liquids on the solid supported lipid bilayers were conducted using GBX Contact Angle Meter (France) by means of the sessile droplet method. In order to measure the advancing contact angle a 3  $\mu$ l droplet from a microsyringe was gently placed on the surface using an automatic deposition system. The contact angle value was evaluated from the 2D shape of settled droplet on its left and right side by the computer program WinDrop++. The measurements were carried out in a closed and humidity-controlled chamber at 20°C and 37°C. The temperature was maintained by the water circulation system. Three independent series of the measurements were conducted for each system.

#### Surface free energy determination

The apparent surface free energy of the bilayers was determined from the Lifshitz-van der Waals – Acid-Base (LWAB) approach as described in the Introduction section.

#### Atomic force microscopy (AFM) measurements

The imaging was carried out using ScanAsyst-HR imaging mode at room temperature with a Nanoscope V (Veeco, USA). In the ScanAsyst-HR mode the tip was forced to oscillate in the  $z$  direction above the sample and touched its surface periodically which allowed direct control of the tip-sample interaction force at ultra-low level. This also protected samples to be not destroyed. Typical image acquisition settings were following: scan angle: 0° and scan speed: 2

Hz. The images were taken with ScanAsyst-HR tip (Bruker) having a spring constant of 0.4 N/m and a resonance frequency between 50 and 90 kHz. The surfaces of 1 $\times$ 1  $\mu$ m<sup>2</sup> were scanned on the center of the sample to avoid edge effect. Analysis of AFM images was performed by using WSxM software.<sup>19</sup> The AFM imaging was conducted in the Faculty of Chemistry Laboratory of our University, with accreditation certificate No. AB 1548.

## Results and discussion

#### Topography analysis

It is recommended that for contact angle measurements the solid surface should be prepared as smooth as possible. The studied bilayer surfaces were characterized by determining the roughness parameters<sup>20</sup> from obtained AFM images. These bilayer surface images are presented in Fig. 2, together with the height profiles tracked along the marked lines (from top left to bottom right) and the height distributions over the entire surface. The values of topographical parameters, i.e. average roughness ( $R_a$ ) (an arithmetic mean deviation of the roughness irregularities from the mean line), root-mean-squared roughness ( $R_q$ ) and average height ( $H_a$ ) are also shown.

In the case of pure DOPC bilayer and DOPC/Chol bilayers at  $x_{\text{Chol}} = 0.25$  and 0.5, the replicas display very smooth and homogeneous surfaces. On the other hand, for the DOPC/Chol bilayer at  $x_{\text{Chol}} = 0.75$  the phase separation takes place and precipitated cholesterol aggregates are seen. They confirm that at this specific DOPC/Chol bilayer stoichiometry, i.e. 1:3, Chol exceeds its solubility limit in the DOPC bilayer and its excess precipitates out and the phase separation within the membrane occurs. Also, the images prove that the Chol bilayer is not continuous (lamellar) because the Chol molecules are rearranged to form islands on the mica surface (Fig. 2). For the homogeneous bilayers, where the Chol aggregates are not present, the height profiles reveal strictly narrow range of the height changes which oscillate around 0.25 nm. The height distributions over the entire surfaces are also narrow with maxima corresponding to the values of average height ( $H_a$ ). This proves high flatness and compactness of the bilayers. Because no holes in the bilayer structures can be found, therefore, it is hardly possible to determine the bilayer thickness from the height profiles. Appearance of the cholesterol aggregates/domains at  $x_{\text{Chol}} = 0.75$  dramatically changes the height profile and distribution. The profile of the surface along the marked line shows a few distinct height levels, i.e. about 1.5–3 nm, 9–12–15 nm, and these thicknesses are approximately those of Chol mono-bilayer, and 3–4–5 Chol bilayers, respectively. It can be also distinguished two height regions over the entire surface, i.e. 1.5–3 nm (major) and 9–12 nm (minor). Hence, the  $H_a$  value does not correspond to the highest number of events but, due to averaging, it is higher.

The analysis of  $R_a$  and  $R_q$  parameters indicates that Chol aggregates precipitation from the DOPC/Chol matrix causes the surface roughness increase (Fig. 2). Both  $R_a$  and  $R_q$  of the pure DOPC and the mixed DOPC/Chol bilayers before the phase separation are low indicating for tightly packed films. However, with the increasing Chol amount in the DOPC bilayer, both parameters decrease. Their minimal values appear at 0.5 molar ratio of Chol. Hence, at this stoichiometry the smoothest films are obtained.

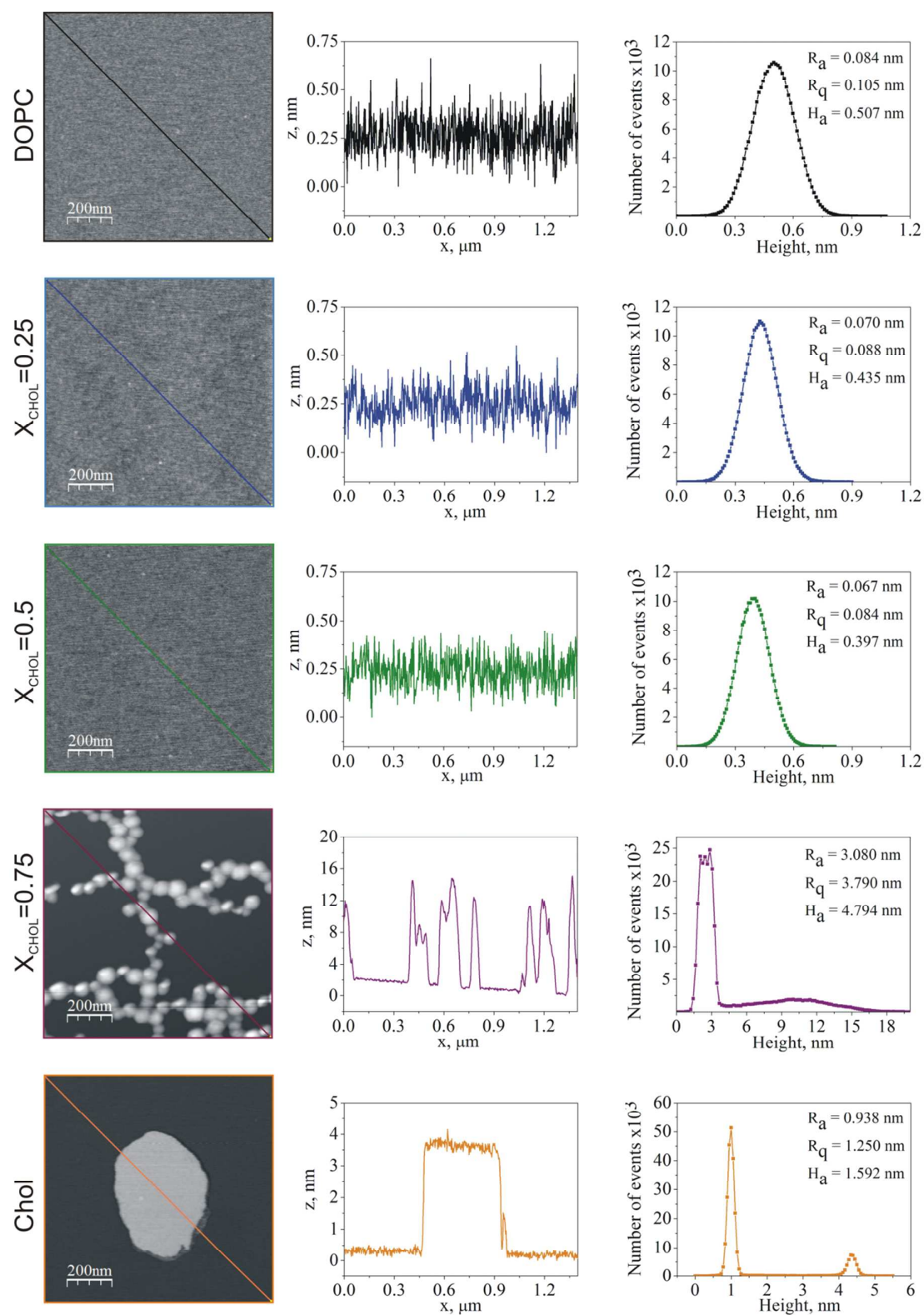


**Fig. 2** 2D AFM images of  $1 \mu\text{m}^2$  surfaces of the DOPC bilayer, DOPC/Chol bilayers at different Chol molar ratio, i.e.  $X_{\text{Chol}} = 0.25, 0.5, 0.75$ , and Chol bilayer, together with the height profiles tracked along the marked lines (from top left to bottom right) and the height distributions.

These results are also in line with those previously reported<sup>21</sup> which indicated that the strongest interactions between the DOPC and Chol molecules occurred at 1:1 stoichiometry ( $x_{\text{Chol}}=0.5$ ). This strong association improves the film condensation and smoothing. However, exceeding the limit of cholesterol solubility leads to the phase separation, hence small domains embedded in the lipid matrix are observed (Fig. 2) and therefore the drastic increase in the  $R_a$  and  $R_q$  values is seen, but the  $R_q$  increase is bigger than that of  $R_a$ . This is because the  $R_a$  depends only on the average profile of heights without distinction between peaks and valleys while the  $R_q$  is more sensitive to peaks and valleys due to the squaring of the amplitude in its calculation.<sup>22</sup> Hence, the  $R_q$  is a more sensitive parameter to describe films with the Chol aggregates. However, these nanometer changes in the film surface roughness are not clearly seen in contact angle changes of the probe liquids (Fig. 3), although it causes changes in the surface free energy. But change in chemical nature of the film (pure Chol) reflects in the contact angle changes (Fig. 3).

### Contact angles

The advancing contact angles of probe liquids on mica supported pure DOPC or Chol bilayers, and mica covered by mixed DOPC/Chol bilayers of different Chol molar ratio, are plotted in Fig. 3. The presence of Chol in the DOPC bilayer causes some changes in the contact angles and a small minimum appears at  $x_{\text{Chol}}=0.5$  (Fig. 3). Generally, the contact angles of polar water (Fig. 3) are higher than those of diiodomethane (except for the cholesterol). Diiodomethane is an apolar liquid whose interactions are almost totally of dispersive nature. Therefore, the contact angles of diiodomethane provide information about the strength of dispersive interactions of the lipid surface. The measured values of advancing water contact angle on various DOPC/Chol bilayers were in the range of 63.1 to 72.2°, however the biggest advancing contact angles of water were obtained on the pure DOPC films at both temperatures.

Keeping in mind strong polar nature of water, its relatively high contact angles clearly indicate apolar nature of the films where the apolar tails of their molecules are easily accessible for polar molecules of the water. Moreover, the contact angles of water and formamide on pure Chol bilayer are much lower than those on the DOPC or DOPC/Chol bilayers. This confirms that cholesterol after transferring onto the solid support does not form uniform lamellar structures (Fig. 2) and hence patches of bare polar mica surface are accessible for polar liquids. On the other hand, the biggest influence of temperature on the contact angles can be seen for pure DOPC and DOPC/Chol (at  $x_{\text{Chol}}=0.25$ ) bilayers. From the analysis of contact angles (Fig. 3), one can conclude that generally wettability of these binary films deposited on mica is determined by their stoichiometry and temperature. A great difference in the wettability, as determined by contact angles of polar liquids, is between pure DOPC and Chol bilayers, where the latter is much more wettable. However, the difference is much less in the case of apolar diiodomethane (Fig. 3). However, the contact angles themselves allow only for a rough-characteristics of the hydrophilic/hydrophobic character of the studied films. More information on the wetting properties of the mixed bilayers can be obtained calculating from the contact angles surface free energy and its components using the theoretical approaches.

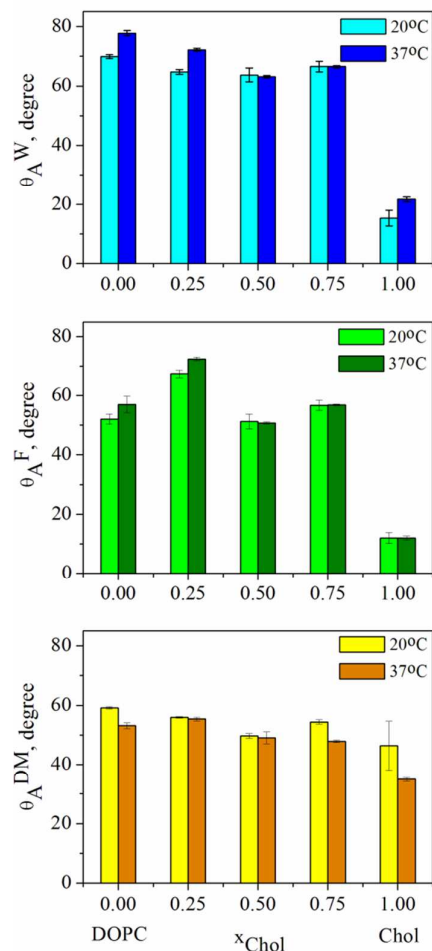


Fig. 3 Advancing contact angles of water ( $\theta_A^W$ ), formamide ( $\theta_A^F$ ) and diiodomethane ( $\theta_A^{DM}$ ) measured on DOPC/Chol bilayers at 20°C and 37°C as a function of cholesterol molar ratio ( $x_{\text{Chol}}$ ).

### Surface free energy and its components of the lipid films

Using Eqs. 1 and 2 and the contact angles from Fig. 3 the apolar Lifshitz-van der Waals  $\gamma_S^{LW}$  and the polar Lewis acid-base  $\gamma_S^{AB}$  component (the electron-donor  $\gamma_S^-$  and electron-acceptor  $\gamma_S^+$  parameters) were calculated. Then total value of the surface free energy was obtained (Eq. 1).<sup>13-16</sup> The values of  $\gamma_L^{LW}$ ,  $\gamma_L^+$ , and  $\gamma_L^-$  of the used probe liquids were taken from the literature (Table 1).<sup>15,17,18</sup> It is commonly accepted that surface tension of apolar diiodomethane results solely from Lifshitz-van der Waals intermolecular interactions and  $\gamma_L^{LW} = \gamma_L$ .

For the sake of clarity the interactions occurring between molecules of the film (DOPC and Chol) and probe liquids (water, formamide and diiodomethane) are depicted in Fig. 4. The DOPC molecule consists of the apolar oleic acid chains and polar glycerophosphocholine head, while the cholesterol molecule possesses only one polar OH group, one double bond ( $\pi$  electrons), and a large apolar sterol ring. The apolar moieties can interact generally by the Lifshitz-van der Waals forces, actually mostly by London dispersion forces. The polar moiety of the DOPC molecule is neutral, i.e. does not bear net electric charge, but possesses charged groups: negative

( $-\text{OPO}_3^-$ ) and positive ( $-\text{N}^+(\text{CH}_3)_3$ ) (zwitterion), as well as several electron-donor oxygen atoms. These regions can interact both by the electron-donor and/or electron-acceptor interactions. The cholesterol molecule possesses only hydroxyl group which can be either an electron-donor or acceptor. Both lipids may interact each other and with liquids used for contact angle measurements. Any polar groups on the DOPC molecule can form  $\text{O}-\text{H}\cdots\text{O}$  or  $\text{C}-\text{H}\cdots\text{O}$  hydrogen bonds with  $-\text{OH}$  of cholesterol, and water (formamide) molecule can form hydrogen bond ( $\text{O}-\text{H}\cdots\text{O}$  or  $\text{C}-\text{H}\cdots\text{O}$ ) with DOPC and/or Chol (Fig. 4).

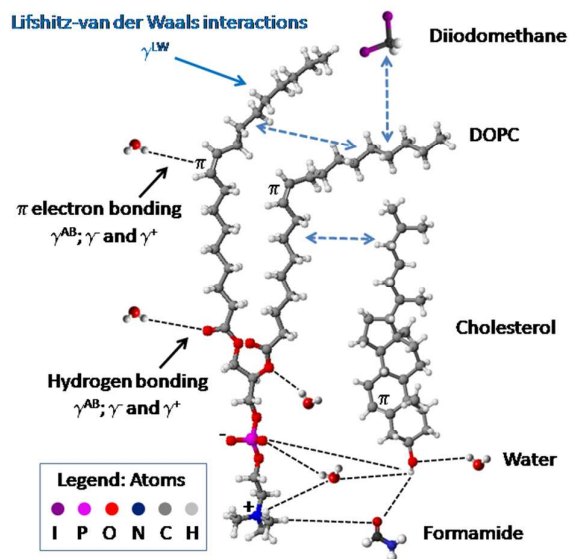


**Fig. 4** Scheme of interactions occurring between DOPC, Chol and probe liquids: water, formamide and diiodomethane.

Having calculated values of the surface free energy, the effect of cholesterol on DOPC bilayers wetting properties can be quantitatively described in terms of changes of the bilayers apparent surface free energy and its components. The results of calculated surface free energy of the studied bilayers at  $20^\circ\text{C}$  and  $37^\circ\text{C}$  are plotted in Fig. 5.

As could be expected the apparent surface free energy of DOPC/Chol bilayers at both temperatures depends on the cholesterol content. Generally, the energy at  $20^\circ\text{C}$  is a little bigger than  $37^\circ\text{C}$ , which is understandable because at the higher temperature thermal energy of the molecules is higher, which affects the interactions. The increased temperature influences also structure of the lipid bilayer which manifests through the disordering of the hydrocarbon chains. The DOPC bilayer exists in the disordered liquid-crystalline (fluid) phase because its main phase transition (gel/fluid) takes place at  $-18^\circ\text{C}$ .<sup>23,24</sup> Therefore, the DOPC unsaturated hydrocarbon chains being already disordered at room temperature, their structure is less affected by increasing temperature.<sup>25</sup> The embedding of cholesterol into a liquid-disordered phase increases ordering of the lipid chains and causes formation of the liquid-ordered phase.<sup>11</sup> In addition, the area per lipid molecule is also less temperature dependent. This limited effect of temperature on the area per lipid molecule is most

likely energetically favorable for organisms which live in environment of periodic temperature variations.<sup>26</sup>

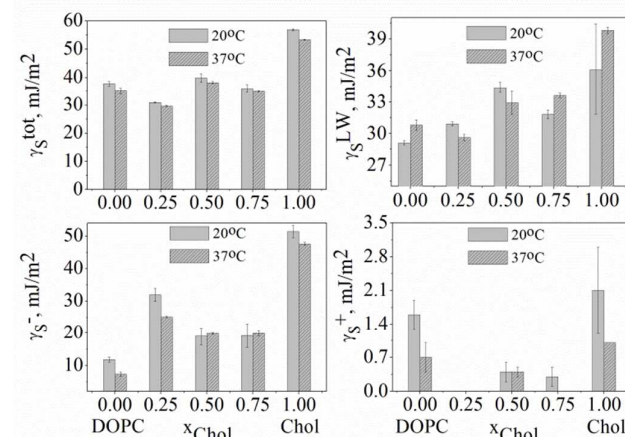


**Fig. 5** Total surface free energy ( $\gamma_S^{\text{tot}}$ ), Lifshitz-van der Waals component ( $\gamma_S^{\text{LW}}$ ), electron-donor ( $\gamma_S^-$ ) and electron-acceptor ( $\gamma_S^+$ ) parameters of DOPC/Chol bilayers at  $20^\circ\text{C}$  and  $37^\circ\text{C}$  calculated from the LWAB approach depending on cholesterol molar ratio ( $x_{\text{Chol}}$ ).

From Fig. 5 is seen that small amount of cholesterol ( $x_{\text{Chol}} = 0.25$ ) slightly decreases the total apparent surface free energy of the bilayer relative to that of pure DOPC bilayer but its larger contents cause the energy increase. However, the changes of total apparent surface free energy can be less informative than the changes of its components. This is one of the shortages of this model mentioned earlier and results from Eqs 1 and 2. Generally, the changes of the apolar  $\gamma_S^{\text{LW}}$  interaction are small (here within  $5 \text{ mJ/m}^2$ ), which is a generic property of the matter.<sup>13-16</sup>

On the other hand, in most real systems the  $\gamma_S^-$  component is big and  $\gamma_S^+$  is generally small, which is the case also here (Fig. 5). The changes of electron-donor  $\gamma_S^-$  parameter can be significant and they reflect mostly hydrogen bonding. The  $\gamma_S^-$  and  $\gamma_S^+$  interactions are complementary and therefore their product in Eq. 1 can decrease if the weak electron-acceptor interaction  $\gamma_S^+$  has further weakened. Hence, the total surface free energy can decrease. Therefore more information about changes of the bilayer interactions can be deduced from the changes in the components of surface free energy and especially the electron-donor parameter  $\gamma_S^-$ . On the lipid film surface this parameter results from the polar groups which act as an electron-donor (i.e. the oxygen atoms are acceptors for hydrogen atoms of water) (Fig. 4). It appears that the biggest electron-donor  $\gamma_S^-$  interaction comes out just if the cholesterol content  $x_{\text{Chol}} = 0.25$ , while the calculated apparent total free energy is the lowest. Here, this is caused by weakened the electron-acceptor  $\gamma_S^+$  interactions, both of the polar DOPC head and  $-\text{OH}$  polar group of cholesterol. Because the  $\gamma_S^+$  and  $\gamma_S^-$  interactions are complementary (Eq. 1),<sup>13-16</sup> therefore the acid-base interaction, i.e. their product, see Eq. 1, practically does not contribute to the total surface free energy, because of nearly zero  $\gamma_S^+$  value (Fig. 5). However, the acid-base parameters interact individually with complementary parameters of probe liquids. Therefore, the changes of individual parameters of the apparent surface free energy shed more light on changes of the bilayer wetting property than its total value. As it can be seen in

Fig. 5 the electron-donor  $\gamma_S^-$  plays important role in the interfacial interactions which is however 'hidden' if the total value of the apparent surface free energy is analyzed. The increased  $\gamma_S^-$  interaction of DOPC bilayer with cholesterol molecules must result from easier and profound their contact with the polar probe liquids (water and formamide). Because cholesterol itself does not bear any strong  $\gamma_S^-$  interaction ( $\gamma_{Chol}^- = 2 - 6 \text{ mJ/m}^2$ ),<sup>27</sup> the observed significant increase of this component already at small content of cholesterol,  $x_{Chol}=0.25$  in the DOPC bilayer (Fig. 5), suggests that some reorganization of the molecules takes place. Moreover, because the dried pure DOPC bilayer deposited on mica shows small electron-donor interaction (Fig. 5), it means that polar water and formamide molecules have limited access to the polar head on such bilayer. In other words, the heads are hidden and/or screened by the hydrocarbon tails.

Quoting some literature results is helpful to understand the energy changes. The unsaturated double bond in the alkyl chain lowers water penetration into the bilayer but incorporation of cholesterol (30 mol%) decreases hydrophobicity and increases water penetration down along the polar headgroups to the location of rigid steroid ring of cholesterol.<sup>28</sup> Both double bonds in the phospholipid chains and intercalation of Chol inside the bilayer make the distance between PC-headgroups larger. Hence the interactions between polar groups become weaker. The carbonyl and phosphate oxygen atoms become easier accessible to water and the hydration increases via hydrogen bonds.<sup>29</sup> The area per lipid molecule for fully hydrated DOPC amounts  $72.2 \text{ \AA}^2$ ,<sup>30</sup> which is considerably larger than that of partially hydrated ( $59.4 \text{ \AA}^2$ ).<sup>31</sup> These data well explain great increase of the electron-donor  $\gamma_S^-$  interaction at  $x_{Chol}=0.25$  seen in Fig. 5. The AFM analysis shows that the  $\gamma_S^-$  increase is not caused by the surface roughness changes (Fig. 2), but rather is due to looser the bilayer region accessible for the liquids. However, with increasing amount of cholesterol the tilt angle of its molecules relative to the bilayer normal decreases, and the compression of acyl chains of the phospholipid takes place.<sup>32</sup> In consequence the bilayer thickness initially increases, up to  $x_{Chol} = 0.35$ , and then at a higher cholesterol molar fraction it decreases due to the movement of DOPC headgroups. This reflects in the decrease of average height of protrusions as well as  $R_a$  and  $R_q$  parameters (Fig. 2), i.e. the bilayer becomes smoother. The bilayer surface free energy components at  $x_{Chol} = 0.5$  correspond to the situation when the DOPC head groups are less stiff. This may appear in a decreased electron-donor interaction relative to that at  $x_{Chol}=0.25$  (Fig. 5). At  $0.67 \pm 0.02$  molar fraction of cholesterol in DOPC bilayer its solubility limit occurs<sup>32-34</sup> and the acyl chains of DOPC molecules become more disordered when the maximum solubility of cholesterol is reached.<sup>32</sup> If the cholesterol amount still increases its microcrystals are formed (excess cholesterol precipitates from the bilayer) and the lipid packing in the bilayers becomes less ordered.<sup>33,35</sup> Thus cholesterol distributes into two different coexisting domains: phospholipid/cholesterol and cholesterol bilayer.<sup>4</sup> The surface free energy components at  $x_{Chol}=0.75$  (Fig. 5) reflect the situation where DOPC bilayer is 'saturated' with cholesterol and its microcrystals coexist. However, the results in Fig. 5 show that the presence of these domains does not practically affect the electron-donor interaction in comparison to that at  $x_{Chol} = 0.5$  presence, despite the increased surface roughness. As was mentioned above, this is

because cholesterol itself possesses very weak electron-donor interactions. Moreover, cholesterol has a rigidifying effect only to the depth occupied by the rigid structure of its steroid-ring, and fluidizing effect at deeper locations was observed.<sup>4,28</sup> Hence at saturating amounts of cholesterol in the membranes there is characteristic rectangular shape of the hydrophobicity profile across the phospholipid/cholesterol domain with its abrupt change occurring between carbon atom C9 and C10 positions, i.e. location of the steroid-ring in the membrane. The saturating amount of cholesterol increases the hydrophobic barrier for polar molecules in central part of the membrane and also increases the rigidity barrier for nonpolar molecules near the membrane surface.<sup>4</sup> Furthermore, our findings are in agreement with the studies of Starov and Velarde<sup>36</sup> who found that static advancing contact angles are not affected by the surface protrusions if their heights are less than 10-30 nm, i.e. in consequence the apparent surface free energy and its components.

To summarize, it is well known that depending on cholesterol content in DOPC films the changes in packing, ordering of the bilayer and tilting of cholesterol molecules occur, and these all influence the bilayer permeability. The more permeable is bilayer the easier is penetration of a polar probe liquid into the layer interior. Hence such liquid like water or formamide can easier interact with the lipid molecules by hydrogen bonds, and hence significant increase in the electron-donor component of DOPC/Chol bilayer surface free energy takes place (up to  $20 \text{ mJ/m}^2$ , Fig. 5). However, the biggest DOPC/Chol polarity of the bilayer results at low cholesterol content  $x_{Chol} = 0.25$ , when probably the biggest changes in the bilayer ordering occur.

## Conclusions

The studies provided detailed information on the changes of the apparent surface free energy of the DOPC/Chol films of different Chol amounts at 20°C and 37°C. The results demonstrate that the presence of cholesterol in the supported DOPC bilayer affects its apparent surface free energy, especially the electron-donor parameter resulting from hydrogen bonding with the phospholipid polar group. However, the changes are not linearly depended on the cholesterol content. The obtained results show that the membrane composition and temperature determines the hydrophobic/hydrophilic properties of the model membranes. It was found that the changes in the surface free energy components are not directly related to the film roughness of nanometer scale. However, the contact angles are sensitive to the changes of chemical nature of the film and its structure, that is pure Chol layer.

## Acknowledgements

Support from Marie Curie Initial Training Network "Complex Wetting Phenomena" (Project number 607861) is highly appreciated.

## References

- 1 H. Ohvo-Rekilä, B. Ramstedt, P. Leppimäki and J.P. Slotte, *Prog. Lipid Res.*, 2002, **41**, 66.
- 2 T. Róg, M. Pasenkiewicz-Gierula, I. Vattulainen and M. Karttunen, *Biochim. Biophys. Acta*, 2009, **1788**, 97.
- 3 J. Huang and G.W. Feigenson, *Biophys. J.*, 1999, **76**, 2142.
- 4 W.K. Subczynski, M. Raguz, J. Widomska, L. Mainali and A. Kononov, *J. Membrane Biol.*, 2012, **245**, 51.
- 5 R.F. Jacob, R.J. Cenedella and R.P. Mason, *J. Biol. Chem.*, 1999, **274**, 31613.
- 6 R.P. Mason, T.N. Tulenko and R.F. Jacob, *Biochim. Biophys. Acta*, 2003, **1610**, 198.
- 7 L. Huang, V. Grami, Y. Marrero, D. Tang, M.C. Yappert, V. Rasi and D. Borchman, *Invest. Ophthalmol. Vis. Sci.*, 2005, **46**, 1682.
- 8 S.L. Veatch, O. Soubias, S.L. Keller and K. Gawrisch, *Proc. Natl. Acad. Sci. U. S. A.*, 2007, **104**, 17650.
- 9 S. Mabrey and J.M. Sturtevant, *Proc. Natl. Acad. Sci. U. S. A.*, 1976, **73**, 3862.
- 10 T. Baumgart, S.T. Hess and W.W. Webb, *Nature*, 2003, **425**, 821.
- 11 M. Eeman and M. Deleu, *Biotechnol. Agron. Soc. Environ.*, 2010, **14**, 719.
- 12 E. Plesnar, W.K. Subczynski and M. Pasenkiewicz-Gierula, *Biochim. Biophys. Acta*, 2012, **1818**, 520.
- 13 C.J. van Oss, M.K. Chaudhury and R.J. Good, *Chem. Rev.*, 1988, **88**, 927.
- 14 C.J. van Oss, R.J. Good and M.K. Chaudhury, *J. Colloid Interface Sci.*, 1986, **111**, 378.
- 15 C.J. van Oss, W. Wu, A. Docoslis and R.F. Giese, *Colloid Surf. B*, 2001, **20**, 87.
- 16 C.J. van Oss, *Colloids Surf. A*, 1993, **78**, 1.
- 17 C.J. van Oss, R.J. Good and H.J. Busscher, *J. Dispersion Sci. Technol.*, 1990, **11**, 75.
- 18 A.M. Gallardo-Moreno, M.L. González-Martin, J.M. Bruque and C. Pérez-Giraldo, *Phys. Chem. Chem. Phys.*, 2004, **6**, 1512.
- 19 I. Horcas, R. Fernandez, J.M. Gomez-Rodriguez, J. Colchero, J. Gomez-Herrero and A.M. Baro, *Rev. Sci. Instrum.*, 2007, **78**, 013705. (2007).
- 20 E.S. Gadelmawla, M.M. Koura, T.M.A. Maksoud, I.M. Elewa and H.H. Soliman, *J. Mater. Process. Technol.*, 2002, **123**, 133.
- 21 M. Jurak, *J. Phys. Chem. B*, 2013, **117**, 3499.
- 22 www.intechopen.com
- 23 R.N.A.H. Lewis, B.D. Sykes and R.N. McElhaney, *Biochemistry*, 1988, **27**, 880.
- 24 T.P.W. McMullen, R.N.A.H. Lewis and R.N. McElhaney, *Curr. Opin. Colloid Interface Sci.*, 2004, **8**, 459.
- 25 J. Pan, F. A. Heberle, S. Tristram-Nagle, M. Szymanski, J. Katsaras, Norbert Kučerka and M. Koepfinger, *Biochim. Biophys. Acta*, 2012, **1818**, 2135.
- 26 J.R. Hazel and E.E. Williams, *Prog. Lipid Res.*, 1990, **29**, 167.
- 27 L. Holysz, A. Szczes and E. Chibowski, *Colloids Surf. A*, 2014, **440**, 49.
- 28 W.K. Subczynski, A. Wisniewska, J-J. Yin, J.S. Hyde and A. Kusumi, *Biochemistry*, 1994, **33**, 7670.
- 29 K. Murzyn, T. Róg, G. Jezierski, Y. Takaoka and M. Pasenkiewicz-Gierula, *Biophys. J.*, 2001, **81**, 170.
- 30 S. Tristram-Nagle, H.I. Petrache and J.F. Nagle, *Biophys. J.*, 1998, **75**, 917.
- 31 M.C. Wiener and S.H. White, *Biophys. J.*, 1992, **61**, 428.
- 32 M. Alwarawrah, J. Dai and J. Huang, *J. Phys. Chem. B*, 2010, **114**, 7516.
- 33 A. Parker, K. Miles, K.H. Cheng and J. Huang, *Biophys. J.*, 2004, **86**, 1532.
- 34 M.R. Ali, K.H. Cheng and J. Huang, *Proc. Natl. Acad. Sci. U.S.A.*, 2007, **104**, 5372.
- 35 J. Huang, J.T. Buboltz and G.W. Feigenson, *Biochim. Biophys. Acta*, 1999, **1417**, 89.
- 36 V.M. Starov and M.G. Velarde, *J. Phys.: Condens. Matter*, 2009, **21**, 464121.